ICANS-XIX,
19$^{\text{th}}$ Meeting of the International Collaboration on Advanced Neutron Sources
March 8–12, 2010
Grindelwald, Switzerland

EXPERIMENTAL INVESTIGATION OF NEW NEUTRON MODERATOR MATERIALS

M. Mocko, L. L. Daemen, M. Hartl, Th. Huegle, G. Muhrer

Los Alamos National Laboratory, P. O. Box 1663, Los Alamos, NM 87545, USA

Abstract

In this study we present experimental investigation of thermal neutron energy spectra produced by lead and bismuth hydroxides ($Pb(OH)_2$, and $Bi(OH)_3$). The experimental energy spectra are compared with a thermal neutron energy spectrum of water measured in the same geometry. We present an MCNPX geometry model used to help with the experimental data interpretation. We demonstrate a very good reproduction of the experimental thermal neutron energy spectrum produced by the water moderator. We show a sensitivity study with the $Pb(OH)_2$ and $Bi(OH)_3$ materials on different combinations of thermal neutron scattering kernels.

1. Introduction

Over the last 40 years thermal and cold neutron production at spallation sources was limited to a few neutron-moderator materials: light water, liquid/solid methane, liquid/solid deuterium and liquid hydrogen. While these materials served the neutron moderation purpose well, the current neutron source designs are reaching the physical limitations of the construction materials. In the past clever design choices have been able to make up for the material shortfalls. However, with increasing demand for stronger and brighter neutron sources and very little room for additional optimizations of the designs, the next-generation neutron sources need to address the fundamental limitations of the currently used materials.

One of the biggest constraints of the moderator materials used today is the limited temperature range where they can be safely operated, which leads to a limited flexibility of the neutron energy spectrum profile. While many of the neutron scattering instruments use thermal neutrons for their operation, in some cases they would prefer a source operated at 150 K, which cannot be achieved with light water because the structure of ice depends strongly on the freezing conditions of water. Even experiments at a given neutron scattering instrument do not necessarily share the preference of the neutron energy spectrum. The added flexibility of "tuning" the maximum of the Maxwellian spectrum could provide added neutron intensity where it is needed the most, accelerating certain experiments or enabling others.

On the other hand, most nuclear physics experiments do not use thermal neutrons at all, because are mostly interested in epi-thermal and fast neutrons. Ideally, material science and nuclear physics instruments should be served by different moderators. However, in reality, they commonly that they share the same neutron moderator [1]. Therefore any moderator design is based on a compromise between many competing constraints and requirements. The present study tried to respond to this challenge by investigating $Pb(OH)_2$ and $Bi(OH)_3$ as potential neutron moderator materials.

2. Investigated neutron moderator materials

It is commonly understood that, in the first approximation, the amount of hydrogen in the material is directly proportional to the thermal neutron brightness of the moderator. On the other hand, high-Z (heavy) materials are commonly preferred when one needs to maximize the epi-thermal neutron flux. From these two simple principles it is clear that we need to consider materials that contain both hydrogen and high-Z elements. However, one needs to keep in mind that many heavy metals have a fairly high absorption cross section, which might adversely affect the thermal neutron flux. Keeping in mind this constraint we considered two elements: lead, and bismuth. Ideally, we would consider hydrates of these elements (PbH_2, BiH_3), but these materials are chemically very unstable and it is difficult to produce them in large enough quantities. We have therefore, started investigating hydroxide forms of these elements: $Pb(OH)_2$, and $Bi(OH)_3$.

Table I: Physical properties and amounts of the investigated materials used in our experimental study.

Material name	Prepared amount (g)	Thickness	Tabular density (g/cm^3)	Prepared density (g/cm^3)
H_2O	N/A	3.0	1.0	1.0
$Pb(OH)_2$	1734	4.6	7.6	4.6
$Bi(OH)_3$	713	2.7	4.4	2.1

Table I summarizes the amounts of investigated materials we used in our experimental study. It is worthwhile noting that the effective thickness of the moderator was similar for H_2O and $Bi(OH)_3$, but we used a substantial amount of $Pb(OH)_2$ in our study.

The experimental study was carried out in the Blue Room, with access to the proton beam, at Los Alamos National Laboratory's Los Alamos Neutron Science Center's (LANSCE's) Weapons Neutron Research facility. A schematic of the experimental layout is shown in Fig. 1. The target setup used in our investigation is a mock-up of the LANSCE's Lujan Center's target-moderator-reflector-shield system [1] with a split tungsten target and a room-temperature beryllium reflector. For the detection of neutrons we used a short vertical flight path with effective length of about 6 m. The investigated moderator materials were encapsulated in aluminum enclosures with thin (2 mm) windows at both the top and the bottom (emission surface). These enclosures were placed below the proton beam axis with a polyethylene moderator directly above (see Fig. 1) in a so-called flux-trap geometry. The whole target-moderator-reflector system was completely coupled. We used eight identical ^{3}He tubes (LND Inc.) for detection of thermal neutrons produced by the investigated moderator material. A series of thirteen borated aluminum collimators and one cadmium ring defined the field of view on the emission surface of the moderator enclosures withe a diameter of 10 cm.

3. Experimental results

The measured thermal neutron energy spectra are presented in Fig. 2. The three investigated systems are shown in different colors: black, red, and blue for H_2O, $Bi(OH)_3$, and $Pb(OH)_2$, respectively. The six panels represent the spectra seen by different detector tubes, numbered from left to right as presented in schematic shown in Fig. 1. At the first glance we see that the spectra produced by H_2O and $Bi(OH)_3$ are very similar in terms of shape and overall intensity and the spectra generated by $Pb(OH)_2$ are in all cases lower in intensity. We also note that the overall intensity varies from detector tube to tube. The thermal neutron intensity increases from tube #1 to #2, reaching a maximum for #3 and then gradually decreases to tube #6. The overall thermal neutron intensity profile is a direct consequence of the detector tube placement, where tube #3 is placed in the middle of the circular beam spot receiving the maximum number of thermal neutrons.

An easy comparison of the neutronic performance of the investigated materials is to calculate the relative thermal neutron flux. We calculated the ratio of the integrated thermal neutron flux produced by the studied hydroxides ($Bi(OH)_3$, $Pb(OH)_2$) and water. Table II presents these ratios for individual tubes in our experiment. We note that the ratios (relative data) do not depend on the detector tube and their placement with respect to the vertical flight path. From Table II we can quantify the relative thermal neutron performance of $Bi(OH)_3$ to be only 6–7% worse than that of H_2O, while the $Pb(OH)_2$ underperforms water by approximately 30–35%. Indeed, it is important to keep in mind that these results were observed in our particular geometry (Fig. 3) and are inherently influenced by our choices of volumes (of the moderator materials) and other arrangements in our experimental setup.

4. Monte Carlo study

To allow for a broader interpretation of the experimental results and their possible application in different circumstances we need to understand the experiment in a modeling (theoretical) study. We used the Monte Carlo MCNPX code [2] package to reproduce our experimental results. In all our calculation we used MCNPX version 2.7.a with the capability of processing the new continuous representation of thermal neutron scattering kernels [3].

In Fig. 3 we present the high-fidelity geometry representation implemented as a 3-dimensional model in MCNPX used for all our calculations. The leftmost snapshot in Fig. 3 shows the entire experimental setup with vertical neutron

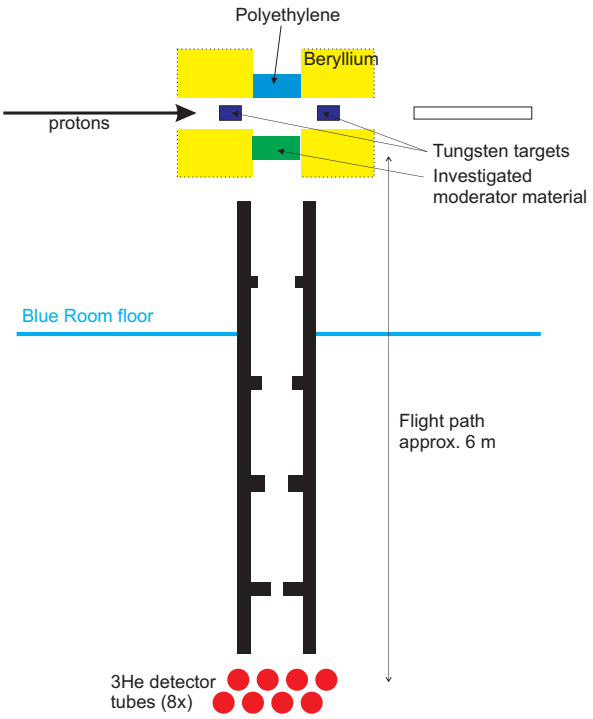

Fig. 1: A schematic of the experimental setup used to investigate the new moderator materials.

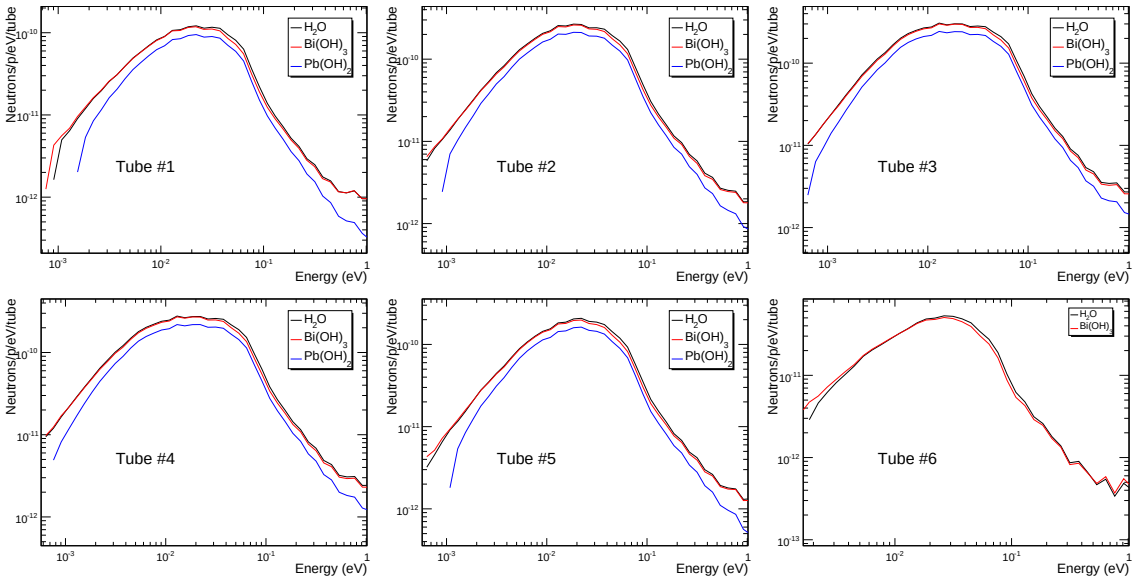

Fig. 2: Experimental thermal neutron energy spectra measured for the three investigated materials: H_2O (black), $Bi(OH)_3$ (red), and $Pb(OH)_2$ (blue)

Table II: Experimental ratios of thermal neutron flux in individual detectors.

Detector #	$Pb(OH)_2/H_2O$	$Bi(OH)_3/H_2O$
1	0.74	0.93
2	0.76	0.94
3	0.77	0.94
4	0.76	0.94
5	0.75	0.93

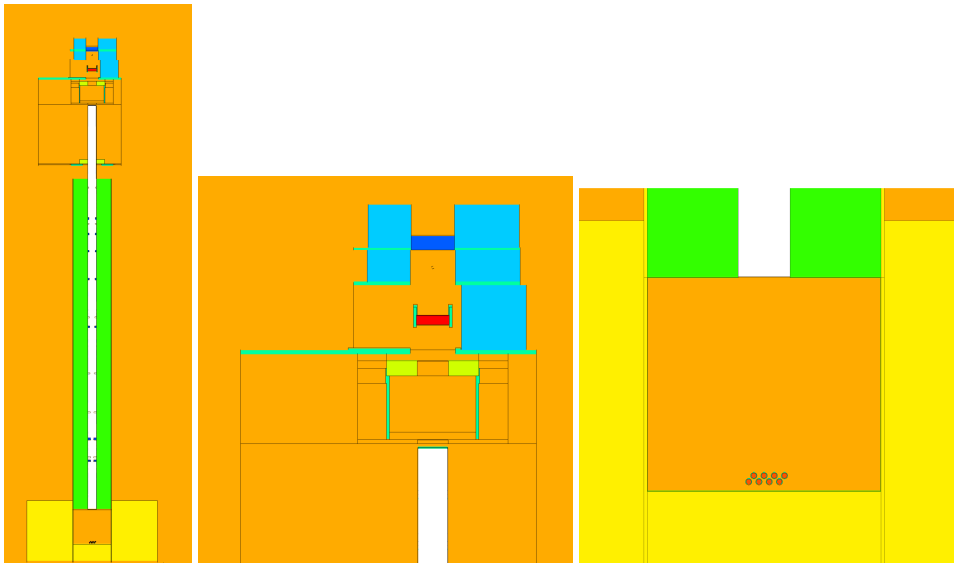

Fig. 3: High-fidelity MCNPX model geometry of the experimental investigation of new moderator materials in the Blue Room.

flight path, middle picture depicts a detailed view of the moderator-reflector assembly with the studied moderator material in red, and the rightmost figure shows a close-up view of the detector tubes and their arrangement.

The MCNPX Monte Carlo calculations are very CPU-intensive, hence one needs to use approximations to have the results converge in a reasonable amount of CPU time. The MCNPX package contains numerous techniques for faster convergence (variance reduction). A very effective technique is called a point detector (F5 tally). It is usually the preferred alternative. But in our case, we needed to show that it does not distort the results; our data were collected in detector tubes not positioned on the axis of the neutron flight path (Fig. 3), but in a plane perpendicular to it. In one case we tallied the neutron energy in the volume (F4 tally) of the detector tubes (as depicted in rightmost picture of Fig. 3). The thermal neutron energy spectrum generated by the F4 tally is plotted in the left panel of Fig. 4 as a red line. In the same plot we compare it to the energy spectrum generated by an F5 tally placed on the axis of the vertical neutron flight path. Both spectra are amplitude-normalized to 100. We notice a much worse statistics for the F4 tally result, but we can conclude that the F5 tally does not distort the spectral shape. Since our study is concerned about reproducing relative quantities we do not need to be worried about the absolute thermal neutron intensities.

The right panel of Fig. 4 presents results of two F5 tallies placed on the axis of the vertical flight path at the detector position. The black line depicts the same spectrum as plotted in the left panel (F5 tally in energy space), the red line represents a spectrum calculated from a time-of-flight (ToF) spectrum generated by an F5 tally (100-μs bin size). Both spectra are amplitude-normalized to 100. In this case, we note that the two spectra exhibit clearly different shapes. The differences are caused by the relatively short flight path (6 m) and the use of a coupled system, resulting in a very low resolution altering the shape of the energy spectrum. Since the experimental data are measured in ToF and then transformed to energy space we need to apply the same procedure to the calculated data.

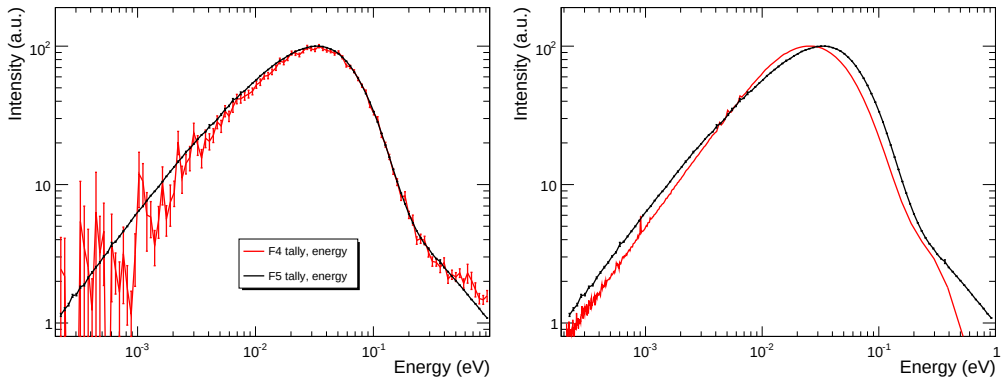

Fig. 4: The left plot provides a comparison of the thermal neutron energy spectra calculated using an F4 tally (neutrons tallied in detector volumes) in red, and an F5 tally (point detector on axis) in black. The plot in the right panel demonstrates different shapes of thermal neutron energy spectra when tallied in energy (black) and ToF (red) space.

In Fig. 5 we compare the measured (red) and calculated (black) thermal neutron energy spectra produced by H_2O. Both the experimental and the calculated results are transformed from ToF to energy in the same fashion[1]. For convenience, all presented spectra are amplitude-normalized to 100. Clearly the experimental spectra differ depending on detector tube number. We note a very good agreement, between the experimental and calculated spectra, for tubes #1, #2, #5, and #6, while the experimental energy spectra seen by tubes #3, and #4, exhibit a much broader shape. We believe that the differences in terms of the energy spectrum shape are caused by insufficient shielding around the detectors at the time of the experiment. During the disassembly of the setup we discovered missing pieces of cadmium sheets on the openings used to access the detector location. The cadmium shielding was missing on the sides at both ends of the detector tubes. It is easy to see how these two openings could contribute to neutron events in the center-most tubes exposed to highest flux, via scattering, thermalization or slowing-down in the neighboring steel shielding blocks. It is interesting to note that the relative thermal neutron flux as shown in Table II does not depend on the neutron detector number. It shows that the relative importance of these unshielded-neutron contributions is probably very similar so it cancels out in the ratios. Fig. 5 demonstrates a very successful reproduction of the experimental data when using a high-fidelity geometry model, new continuous representation of H_2O scattering kernel, and experiment-like ToF-to-energy transformation. All of the energy-spectrum calculation results presented in the remainder of this report have been obtained in the same way.

The calculations with the two new moderator materials ($Bi(OH)_3$, $Pb(OH)_2$) are not as straight-forward as the above mentioned results for H_2O. First, the scattering kernels for them have not been produced. However, we have scattering kernels for most of the constituent elements: hydrogen (in H_2O), lead (in solid lead), and bismuth (in solid bismuth). It is worthwhile stressing that these scattering kernels have not been developed and meant to be used for application in either $Bi(OH)_3$, or $Pb(OH)_2$. Lacking a better alternative we decided to use them in this case.

The total neutron scattering cross section generated from the scattering kernels used in our analysis is presented in Fig. 6. The black line shows hydrogen in H_2O [3], lead is depicted by a blue line [4], and bismuth is shown in red [5]. The total neutron scattering cross sections for lead and bismuth are qualitatively similar, with hydrogen significantly different both qualitatively and quantitatively.

Fig. 7 shows the relative influence of different scattering kernels on the final energy spectrum for $Bi(OH)_3$. In the left panel we notice no difference between using the bismuth scattering kernel (black dashed line) and employing the free gas model (red) for all elements of $Bi(OH)_3$. On the other hand, we note a change of the spectral shape when using hydrogen in H_2O scattering kernel (black dashed line) versus using the free gas model (red). We do not show the calculated results for $Pb(OH)_2$, because they exhibit the exact same behavior.

The plots of relative thermal neutron energy spectra for $Bi(OH)_3$ (right panel) and $Pb(OH)_2$ (left panel) with respect to H_2O are shown in Fig. 8. The experimental data are presented as the area in red, representing the statistical and systematic uncertainties of our measurements, the calculations employing the free gas model are shown as dashed

[1]The experimental results are corrected for efficiency, but the calculated data do not need any additional corrections.

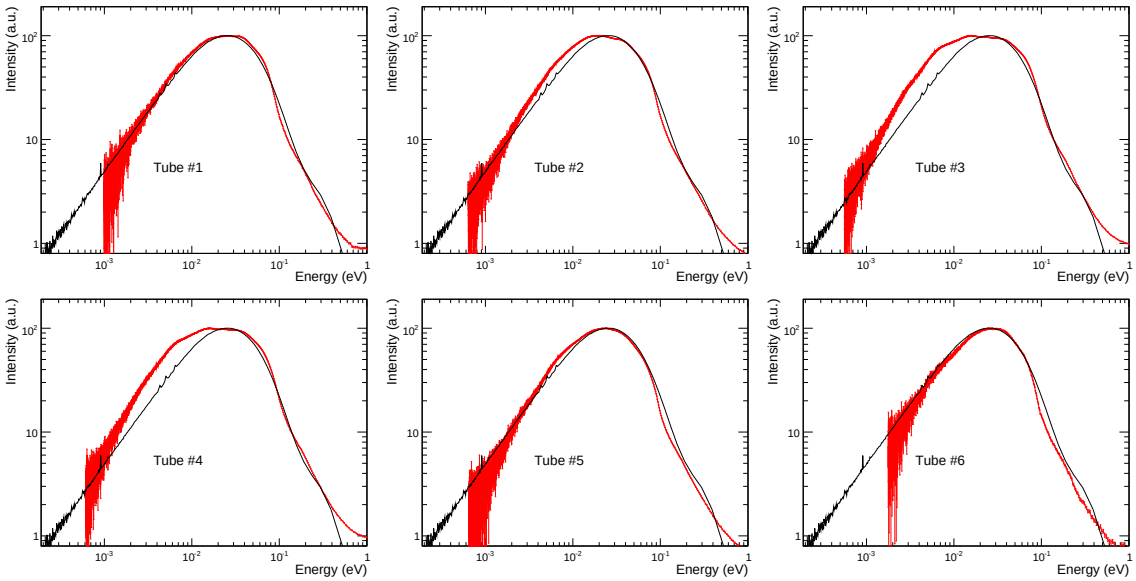

Fig. 5: Comparison of the measured (red) and calculated (black) thermal neutron energy spectra for tubes 1–6.

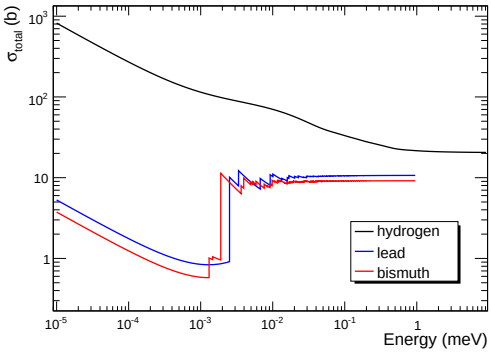

Fig. 6: Total neutron scattering cross section for hydrogen in H_2O (black), lead (blue) and bismuth (red), used in our MCNPX calculations.

lines. The simulations with the hydrogen in H_2O scattering kernel are presented as solid lines. The experimental relative thermal neutron energy spectrum for $Bi(OH)_3$ is relatively flat across the investigated neutron energy range. The relative energy spectrum for $Pb(OH)_2$ on the other hand, has more pronounced features and higher uncertainties towards both ends (mostly caused by lower statistics). The curvature of the experimental ratio in left plot suggests that the thermal neutron spectrum produced by $Pb(OH)_2$ is narrower than that of H_2O.

The use of hydrogen scattering kernels (solid lines) clearly helps to reproduce the experimental data better than the employment of free gas model for the hydrogen atoms in both $Pb(OH)_2$ and $Bi(OH)_3$ cases. However, to fully reproduce the experimental data one would have to develop completely new (effective) scattering kernels for these two materials ($Pb(OH)_2$, $Bi(OH)_3$). Nevertheless, it is worth noticing that the hydrogen atoms behave similarly in H_2O and $Bi(OH)_3$ for a neutron probe.

5. Summary and conclusions

We have prepared samples of $Pb(OH)_2$ and $Bi(OH)_3$ of 1734 g and 713 g, respectively. The thermal neutron spectra produced by H_2O, $Bi(OH)_3$, and $Pb(OH)_2$ have been measured in a coupled geometry (with beryllium re-

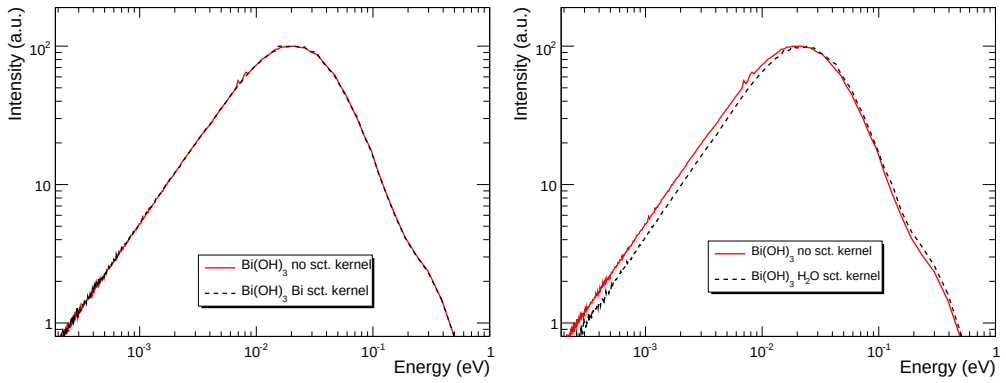

Fig. 7: The left plot shows a that using the bismuth scattering kernel (black) does not differ from using the free gas model (red) for all elemental constituents of $Bi(OH)_3$. The right plot demonstrates a spectrum shift when using the hydrogen in H_2O scattering kernel (black) versus the free gas model (red).

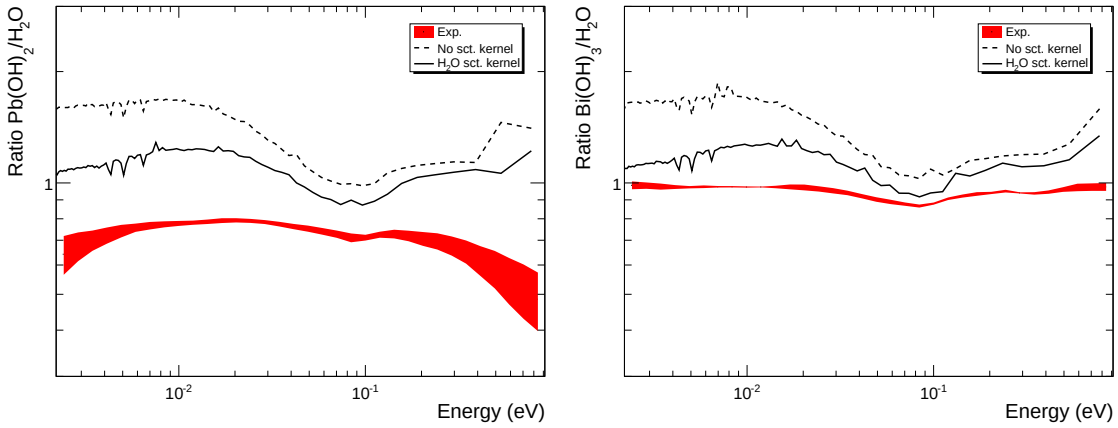

Fig. 8: The relative thermal neutron energy spectra for $Pb(OH)_2$ and $Bi(OH)_3$. The experimental data are plotted as red areas, the dashed lines depict calculations using the free gas model, and the simulations employing the hydrogen in H_2O scattering kernel are shown as solid lines.

flector). The thermal neutron spectrum generated by $Bi(OH)_3$ is very similar in terms of intensity and shape to that of H_2O. The $Pb(OH)_2$ spectrum shows a slightly different shape and approximately 30% lower intensity than that of H_2O.

We demonstrated a very good grasp on understanding the H_2O-generated thermal neutron energy spectra. We could not reproduce the relative energy spectra by using the free gas model for thermal neutron cross sections for $Bi(OH)_3$ and $Pb(OH)_2$. The usage of hydrogen in H_2O scattering kernel provides a slightly better agreement with the experimental data.

6. Acknowledgment

We would like to acknowledge the help and assistance of G. A. Chaparro with the experimental setup in the Blue Room. Also the cooperation of the staff of LANSCE's Central Control Room with the proton beam tune-up and delivery.

References

[1] G. Muhrer, E. J. Pitcher, G. J. Russell, T. Ino, M. Ooi, and Y. Kiyanagi, "Comparison of the measured thermal neutron beam characteristics at the Lujan Center with Monte Carlo transport calculations," *Nuclear Instruments and Methods A*, vol. 527, pp. 531–542, 2004.

[2] LA-CP-07-1473, *MCNPX manual v. 2.6.0*.

[3] http://t2.lanl.gov/data/thermal7.html.

[4] G. Muhrer, T. Hill, F. Tovesson, and E. Pitcher, "Comparison of the measured and the calculated total thermal neutron cross-section of Pb," *Nuclear Instruments and Methods A*, vol. 572, pp. 866–873, 2007.

[5] G. Muhrer, "private communication.".